01 Jan 1993

Collapse Behavior Of Pino Suarez Building During 1985 Mexico City Earthquake

Jeng Fuh Ger

Franklin Y. Cheng
Missouri University of Science and Technology, chengfy@mst.edu

Le Wu Lu

Recommended Citation

J. F. Ger et al., "Collapse Behavior Of Pino Suarez Building During 1985 Mexico City Earthquake," *Journal of Structural Engineering (United States)*, vol. 119, no. 3, pp. 852 - 870, American Society of Civil Engineers, Jan 1993.
The definitive version is available at https://doi.org/10.1061/(ASCE)0733-9445(1993)119:3(852)

COLLAPSE BEHAVIOR OF PINO SUAREZ BUILDING DURING 1985 MEXICO CITY EARTHQUAKE

By Jeng-Fuh Ger,[1] Associate Member, ASCE, Franklin Y. Cheng,[2] Fellow, ASCE, and Le-Wu Lu,[3] Member, ASCE

ABSTRACT: This paper presents the investigation of the collapse behavior of a 22-story steel building during the September 19, 1985, Mexico City earthquake by studying hysteretic behavior, ductility factors of individual structural components, and overall instability of the building. Extensive inelastic analyses have been performed for the building by using the multicomponent seismic input of actual Mexico City earthquake records. It was found that the structural response exceeds the original design ductility of this building, and most girders in the building have severe inelastic deformation. Due to the load redistribution that results from ductile girder failure, local buckling occurred in many columns on floors, 2, 3, and 4. Therefore, most columns on floors 2–4 lost their load-carrying capabilities and rigidities, which then caused the building to tilt and rotate. It is evident that ductile failures of girders combined with local buckling of columns in the lower part of the building resulted in significant story drift, building tilt, P-Δ effect, and the failure mechanism.

INTRODUCTION

The Pino Suarez complex, shown in Fig. 1, was located in the central part of Mexico City and comprised five high-rise steel buildings: three identical 22-story structures and two identical 15-story structures. The structural design and details were the same for all five buildings. The structural systems of the buildings consisted of moment-resisting frames in both N-S and E-W directions and an auxiliary bracing system in one of the bays. The frames were constructed of welded box columns and specially fabricated open-web girders as shown in Fig. 2. The second story was continuous through all five buildings. The lateral design force of these buildings was based on a ductility of four. During the September 19, 1985, Mexico City earthquake, building D collapsed onto building E, and buildings B and C had severe structural damages; building C was close to collapse.

The configuration of this 22-story building is shown in Fig. 3. It contains four bays in the building's long direction (E-W) and two bays in its short direction (N-S). The frame-section numbers, column-line numbers, and story numbers are assigned in this figure. The structure had a two-story penthouse above the braced core; since specific information was not available for use in this study, the penthouse was not included in the structural model.

Several locally buckled columns have been observed in building C. These columns are located on the fourth story at column lines 3, 5, and 6 where large clamps were added after the earthquake to prevent collapse of this building. Local buckling was near the end of the column, and the column plates were no longer connected to each other. As a result, significant

[1]Postdoctoral Fellow of Civ. Engrg., Univ. of Missouri-Rolla, Rolla, MO 65401.
[2]Curators' Prof. of Civ. Engrg., Univ. of Missouri-Rolla, Rolla, MO.
[3]Prof. of Civ. Engrg., Lehigh Univ., Bethlehem, PA 18015.

Note. Discussion open until August 1, 1993. Separate discussions should be submitted for the individual papers in this symposium. To extend the closing date one month, a written request must be filed with the ASCE Manager of Journals. The manuscript for this paper was submitted for review and possible publication on December 9, 1991. This paper is part of the ***Journal of Structural Engineering***, Vol. 119, No. 3, February, 1993. ©ASCE, ISSN 0733-9445/93/0003-0852/$1.00 + $.15 per page. Paper No. 3065.

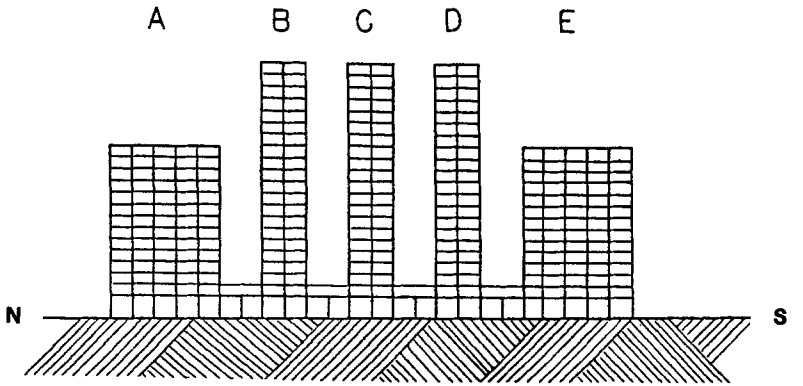

FIG. 1. Pino Suarez Complex

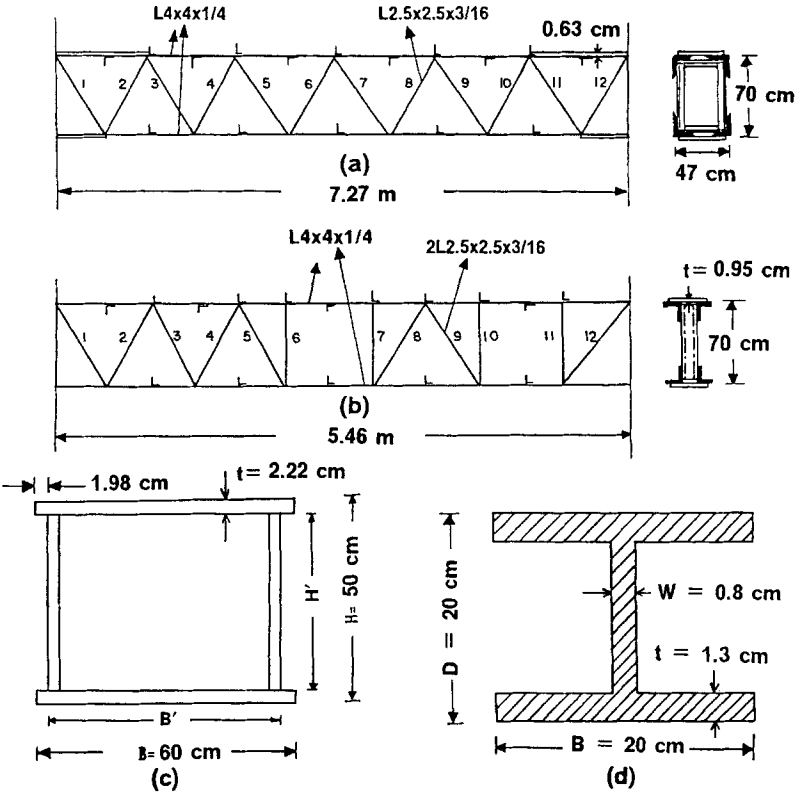

FIG. 2. Typical Structural Members: (*a*) Long-Direction Girder; (*b*) Short-Direction Girder; (c) Welded Box Column; and (*d*) Bracing Member

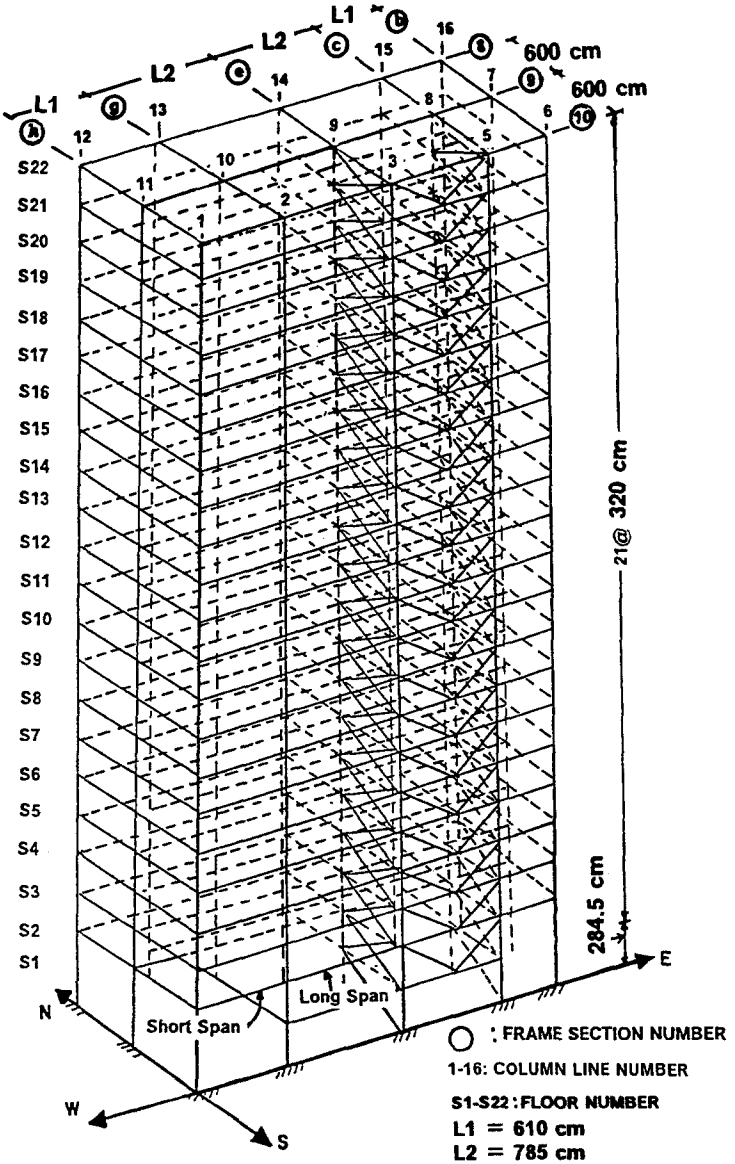

FIG. 3. Configuration of Pino Suarez Building

reductions of axial load and moment capacities can be expected. Also, axial and bending rigidities of the column decrease significantly in the postbuckling stage.

From observation, most long-direction and short-direction girders failed on the lower floors. In short-direction girders, web members showed local buckling at both ends of the members. Some long-direction girders, however, failed because the web members were too weak to resist the shear

forces, leading to overall buckling. Bracing members also exhibited overall buckling.

The seismic response of the Pino Suarez building has been studied by several investigators. Most of the building's structural properties used in their studies are only estimated and not based on actual design information. The hysteretic behavior of the constituent members is based on conventional existing models and is not derived by using the structural properties of the building. Osteraas and Krawinkler (1989) use a two-dimensional structural model in DRAIN-2D (Kannan and Powell 1973) and E-W component earthquake records to study the performance of the building.

The objective of this research is threefold: (1) To study the hysteretic behavior of open-web girders, bracing members, and box columns of the Pino Suarez building; (2) to develop nonlinear hysteresis models of these constituent members; and (3) to use them to investigate the building's performance during the 1985 Mexico City earthquake. Here, a three-dimensional structural model is used in analysis and earthquake E-W, N-S, and vertical components are used as input (Cheng and Kitipitayangkul 1979; Cheng 1980; Ger and Cheng 1992). The structural properties of the Pino Suarez building in this study are based on actual engineering design data.

HYSTERESIS MODEL OF INDIVIDUAL COMPONENT

Long-Direction Long-Span Girders

The hysteresis model of long-direction long-span girders takes a theoretical approach to hysteresis loops of girders (Ger and Cheng 1993). This approach is based on the finite segment formulation with stress-strain control (Chen and Sugimoto 1987; Ger and Cheng 1993; Ger 1990) for angle web members with load eccentricities and initial imperfections. The model is

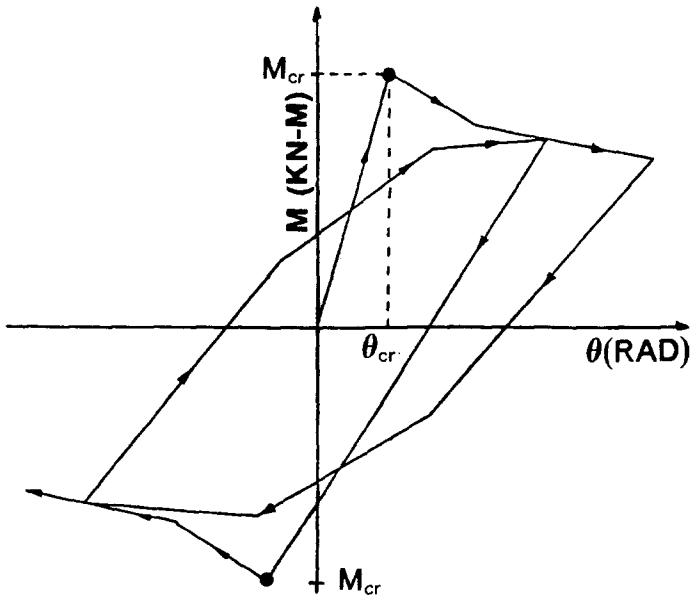

FIG. 4. Hysteresis Model for Long-Direction Girder

sketched in Fig. 4. Using this model, the critical moment M_{cr} and associated rotation θ_{cr} of a girder must first be determined. Coefficients of the stiffness matrix of a girder are then determined according to the rules of the hysteresis model.

Long-Direction Short-Span Girders

The finite segments analysis of the long-direction short-span girders has shown that the girders' hysteretic loops can be treated as bilinear bending hysteresis model (Cheng 1985; Cheng and Ger 1992). The moment of inertia and plastic moment capacity used in this model are based on the cross sections of top and bottom chords only and the effect of web member is ignored. This model assumed that a girder has both a linear and an elastoplastic component. The moments of a girder are a combination of the end moments of these two components according to state of yield. State of yield entails one of the following four conditions: (1) Both ends linear; (2) *i* end nonlinear and *j* end linear; (3) *i* end linear and *j* end nonlinear; and (4) both ends nonlinear.

Short-Direction Girders

In the short-direction girders, web members are box sections made by stitch welding (10 cm at 20 cm) two equal-leg angles together. The overall buckling of each web member is well protected. However, from field observation of building C, some of the web members failed due to local buckling. To investigate the hysteretic behavior of girders, a hysteresis model of web member is first established based on experimental results (Chen 1991) with consideration of hysteresis rules (Jain et al. 1980). The control points in this model are modified to fit experimental results. Using this adjusted model, the hysteretic behavior of the girder is investigated by applying rotational increments to both ends of the girder. This technique is based on the conventional assumption that the first mode dominates the vibration, resulting in antisymmetric deformation of the girder. Since there are two openings in the short-direction girder [Fig. 2(*b*)], the composite effect of concrete slab on top chords must be considered so as not to underestimate the girder's strength The bilinear bending hysteresis model is applied to the top and bottom chords in the analysis. Fig. 5(*a*) shows that the hysteresis loops of short-direction girders are quite stable. Therefore, a simple bilinear hysteresis model is adopted as shown in Fig. 5(*b*). The nonlinear bending

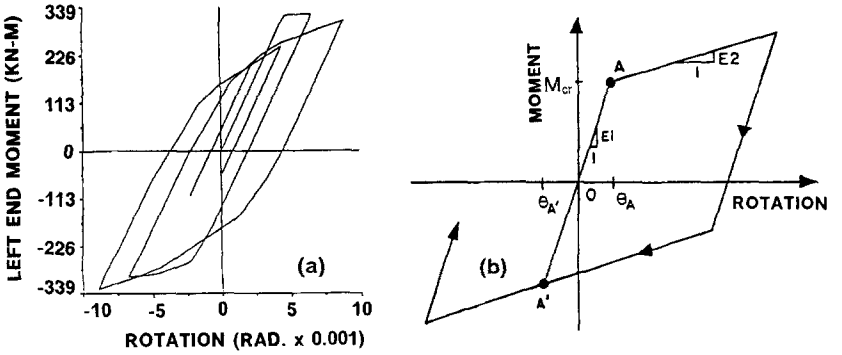

FIG. 5. Hysteresis Loops for Short-Direction Girder: (*a*) Analytical Result; and (*b*) Hysteresis Model

stiffness matrix of the girder is formulated in like manner to that of the long-direction long-span girder. Stiffness coefficients are determined according to the rules in the hysteresis model.

Bracing Members

A bracing system around the building's service core contains two X-braced bays in the structural short direction (in frames c and e) and one K-braced bay in the structural long direction (in frame 10) as shown in Fig. 3. The bracing member consists of three plates welded together into an H shape [Fig. 2(*d*)]. Black et al. (1980) have studied the response behavior of the braces with consideration of the effects of cross-sectional shapes. The study was on the basis of experimental works and the cross-sectional shapes include wide flanges, double angles, double channels, structural tees, pipes, and square tubes. By using Black et al.'s experimental results for wide flanges, the hysteresis rules of Jain et al.'s model (Jain et al. 1980) are then adopted as shown in Fig. 6, with the modification of several control points in Jain et al.'s model to fit the experimental results. The hysteresis loops based on the adjusted model are then compared with the experimental loops. Fig. 7 shows hysteresis loops based on experimental and analytical approaches, respectively, for member W6x20 with slenderness ratio equal to 80. It can be seen that this adjusted model agrees favorably with the experimental loops.

Box Columns

Eight different column sizes are used in the Pino Suarez building. The sizes of these columns are given in Table 1. The limit value of width-thickness ratio for the noncompact box section is $238/\sqrt{F_y} = 39.7$ and the limit value of width-thickness ratio for the compact box section is $190/\sqrt{F_y} = 31.7$, (*Allowable* 1989). F_y represents yielding stress which is equal to 36 ksi (248.22 MPa). Compact sections will not experience local buckling before the formation of a plastic hinge. Noncompact sections will yield first, but local buckling will precede the development of a fully plastic stress distribution. From Table 1, it can be seen that column types C5, C6, C7, and

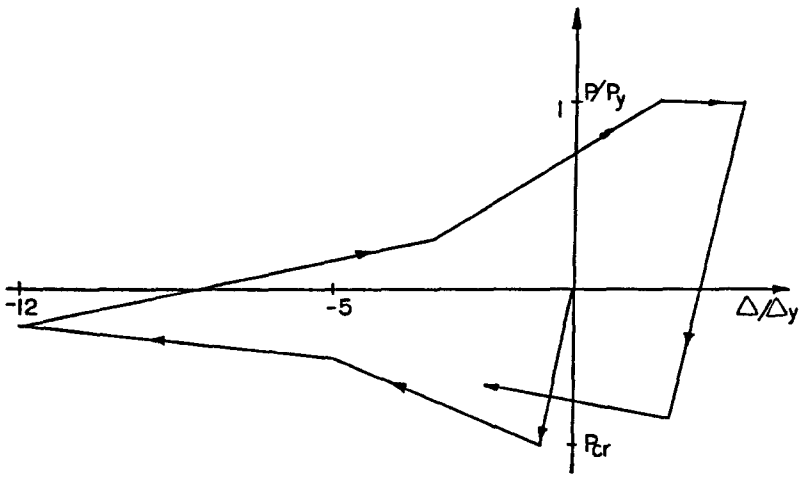

FIG. 6. Hysteresis Model for Bracing Member

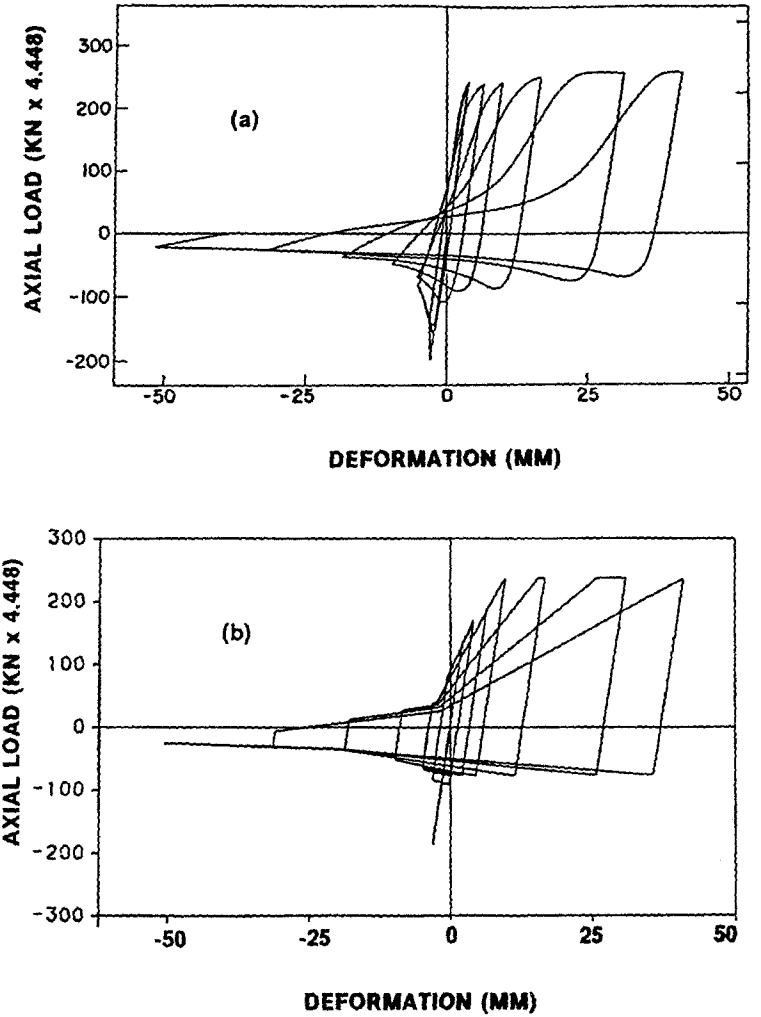

FIG. 7. Hysteresis Loops: (a) Experimental Result (Black et al. 1980); and (b) Analytical Result

C8 are compact sections in which local buckling is minimized, and column types C3 and C4 are noncompact sections in which plate buckling is prevented when stress is just reaching yield stress in compression.

Extensive damages occurred in building C. Most evident is severe local buckling in fourth-story columns 10-b, 10-c, and 10-e (Fig. 3), which are column types C3, C4, and C5, respectively. Although column 10-e was a compact section of C5 type (Table 1), it also buckled locally during the earthquake. Apparently, these columns underwent significant yielding before plates buckled. Axial load combined with bending moments appear to cause severe inelastic deformations in the plates of the box columns. Buckling of these plates results in the failure of welds; this phenomenon is observed from the experimental beam-column tests by Chen (1991).

TABLE 1. Width-Thickness Ratios of Box Columns

Column type (1)	Thickness t (cm) (2)	Flange width B' (cm) (3)	Web width H' (cm) (4)	B'/t (5)	H'/t (6)
C1	0.79	56	48.42	70.88	61.29
C2	0.95	56	48.10	58.94	50.63
C3	1.27	56	47.46	44.09	37.37
C4	1.59	56	46.82	35.22	29.44
C5	1.91	56	46.18	29.32	24.17
C6	2.22	56	45.56	25.22	20.52
C7	2.54	56	44.92	22.04	17.68
C8	3.18	56	43.64	17.61	13.72

Since significant yielding precedes local buckling, the hysteresis model for box columns assumes that local buckling will occur when the cross section of a column reaches its fully plastic condition. The fully plastic condition of a box column can be detected by the following interaction equation for box columns (Zhou and Chen 1985).

$$M_p' = 1.2\left(1 - \frac{P}{P_y}\right) M_p \le M_p \quad \ldots\ldots (1)$$

$$\left(\frac{M_x}{M_{px}'}\right)^{\alpha} + \left(\frac{M_y}{M_{py}'}\right)^{\alpha} < 1 \quad \ldots\ldots (2)$$

$$\alpha = 1.7 - \frac{\dfrac{P}{P_y}}{\ln\left(\dfrac{P}{P_y}\right)} \quad \ldots\ldots (3)$$

where M_p = plastic moment without axial force; M_p' = plastic moment with axial force; and P_y = the axial yield load. When (2) is greater than or equal to one, the cross section of a column reaches the fully plastic condition and local buckling occurs at this stage. The aforementioned criteria are always true only the column's cross section remains compact. It may overestimate local buckling strength of columns with noncompact sections, although a large portion of columns in the lower part of the building are compact sections.

Based on the experimental work of box columns by Liew et al. (1989), a bilinear axial hysteresis model is adopted for evaluating local buckling as shown in Fig. 8. The maximum axial force capacity, P_{cr}, can be determined by whether (2) is greater than or equal to one. When axial force is in compression, axial rigidity in the postbuckling region is assumed to be zero with the column still resistant to residual axial strength. Since axial load capacity drops significantly in the postbuckling region as shown in the experimental results, axial load in this model is reduced from P_{cr} to $\beta' P_{cr}$. When the axial force is in tension, the member resists tension yield load, P_y.

The bilinear bending hysteresis model evaluating local buckling is shown

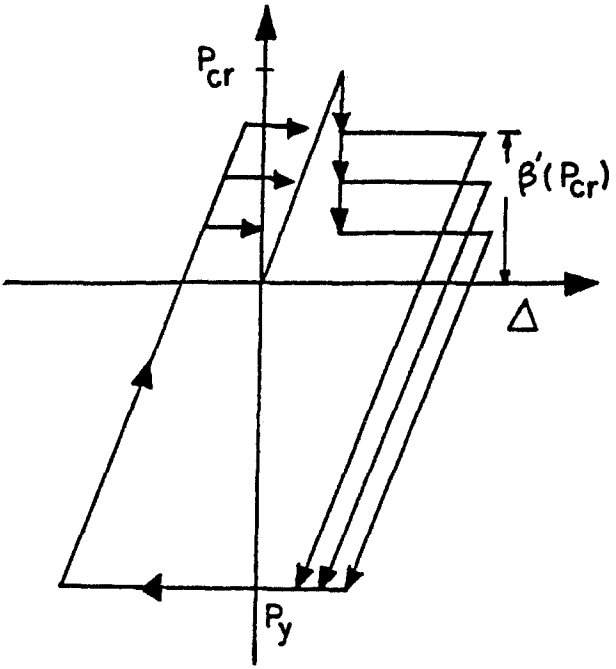

FIG. 8. Axial Load-Deformation Relationships for Local-Buckled Columns

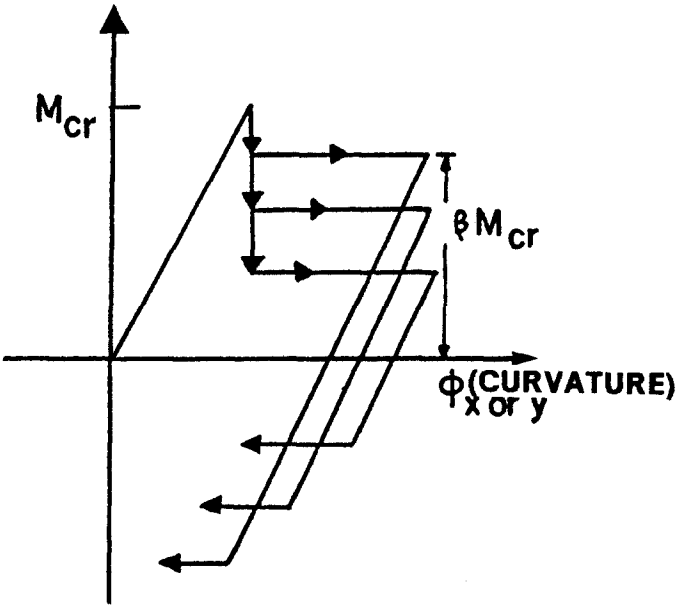

FIG. 9. Bilinear Bending Hysteresis Model Considering Local Buckling

in Fig. 9. Maximum moment capacities along the strong and weak axes, $(M_x)_{cr}$ and $(M_y)_{cr}$, can be determined by letting (2) be greater than or equal to one. Field observations of the Pino Suarez complex and laboratory tests of the prototypic columns (Chen 1991) show that four plates separated due to failed welding caused significant reduction of bending strength. Flexural rigidity in the postbuckling region, then, would be nearly equal to zero with the column still resistant to residual bending strength, expressed as βM_{cr}. Thus, the state of yield for the bilinear bending hysteresis model in the postbuckling region is determined by βM_{cr}.

Structural Model of Pino Suarez Building

The structural model used for the nonlinear analysis of this building is shown in Fig. 10. The global coordinate system (GCS) originates at the ground level. It is assumed that the slab of each floor is rigid in the floor plane and flexible in the out-of-plane direction. Thus, the mass center of each floor can be treated as a master joint with three degrees of freedom, two translations in the X- and Y-directions and one rotation in the Z-direction, and other joints on the same floor can be treated as slave joints.

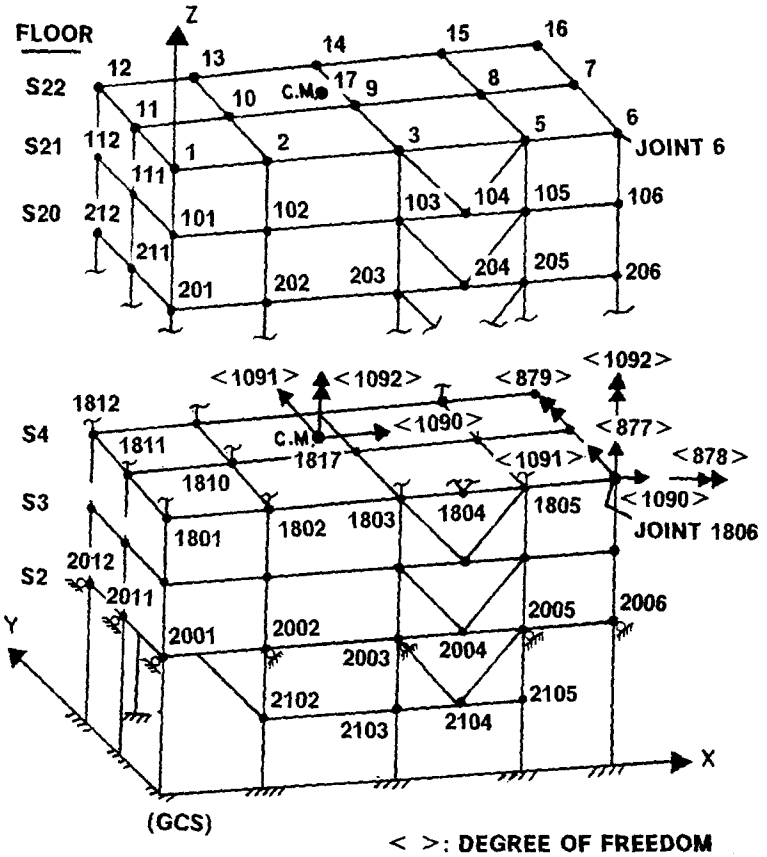

FIG. 10. Structural Model for Pino Suarez Building

Each slave joint has six degrees of freedom in which three degrees of freedom corresponding to two translations in the X- and Y-directions and one rotation in the Z-direction are constrained. Therefore, the degree of freedom numbers at a slave joint's three constrained directions are the same as the degree of freedom numbers at the master joint. As illustrated in Fig. 10, the degree of freedom numbers at master joint 1817 are the same as those at slave joint 1806 in the constrained directions. Since the second story is continuous through all five buildings, the translational degrees of freedom on this floor in the GCS′ X- and Y-directions are restrained. Totally, there are 949 members and 382 joints in this model. The location of a member can be determined by two joints at which the member is connected. According to engineering data, dead load for floors 1–21 is 330.17 kg/m^2 (67.63 psf) and for the roof is 484.78 kg/m^2 (99.3 psf). Live load for floors 1–21 is 350.14 kg/m^2 (71.72 psf) and for the roof is 100 kg/m^2 (20.49 psf). Total static load on a floor is equal to total dead load plus total live load on that floor. Total mass on a floor is equal to total weight on that floor divided by acceleration of gravity. The masses are lumped at the mass center of each floor for translational and torsional excitations. For vertical response, mass is also lumped at each column joint on the floor. Damping ratio is assumed to be 2% of its critical damping. Static load of live and dead load is first applied to the structure. Structure deformations and member internal forces are treated as initial conditions for dynamic analysis. The Wilson-θ approach is adopted for dynamic analysis with $\theta = 1.4$. Time increment is assumed to be 0.01 s. Structural geometric stiffness to account for gravity load and vertical ground motions and unbalanced force are included in the analysis.

Since the location of accelerograph designated as SCT1 is close to the Pino Suarez complex, soil conditions for SCT1 station and this complex are the same. Therefore, SCT1 records with E-W, N-S, and vertical components serve adequately as seismic input for this building. Maximum ground accelerations for E-W, N-S, and vertical components are 167.9, 97.9, and 36.6 gal., respectively. Because the duration of SCT1 records is 180 s, excessive computing time is required for nonlinear dynamic analysis. To economize, only a portion with significant magnitude of each seismic component—40–60 s—is included in time history computation. To ensure the reliability of records 40–60 s in dynamic analysis, these records should mesh with the original records, i.e., 0–180 s. Hence, the acceleration spectrum is used to describe the characteristics of earthquake records. Acceleration spectra 0–180 s are favorably close to acceleration spectra 40–60 s (Ger 1990).

Ductility Definitions

When a structure is subjected to a strong earthquake, the constituent members tend to suffer large deformations. If the members do not have enough ductility, then they will fail and the structure may collapse. The failure ductility most commonly used as the maximum required deformation of a member is

$$\mu_d = \frac{|\delta_{max}|}{\delta_y} \quad (4)$$

where δ_{max} = the maximum deformation of a member; and δ_y = the critical deformation of the member. For a long-direction long-span girder or short-direction girder, δ_y is defined as the end rotation of the member when its

J. Struct. Eng., 1993, 119(3): 852-870

end moment reaches the critical moment, M_{cr}. For a long-direction short-span girder, $\delta_y = M_p L/6EI$ where L is member length, and M_p and EI are the plastic moment and moment of inertia based on the cross sections of top and bottom chords only. If a member reaches its failure ductility, the internal forces of the member will be released and redistributed to adjacent members. Thus, the ductile-failed member can no longer resist a given force. For structures, system ductility can be defined by (4), where δ_y is structural response when the first element of the structure reaches its critical load—i.e., critical moment, plastic moment, or buckling load—and δ_{max} represents the maximum structural response.

Inelastic Response Behavior of Pino Suarez Building

Without Girders' Failure Ductilities and Columns' Local Bucklings

Bilinear bending and axial hysteresis models are used without consideration of column local buckling. From the analysis, most structural members, notably long-direction girders and short-direction girders, went beyond the elastic limit. Structural responses are quite stable and the building does not collapse. In the analysis, member 1413-1414 (the member that has member ends at joint 1413 and joint 1414) is the first to reach its critical load. Thus,

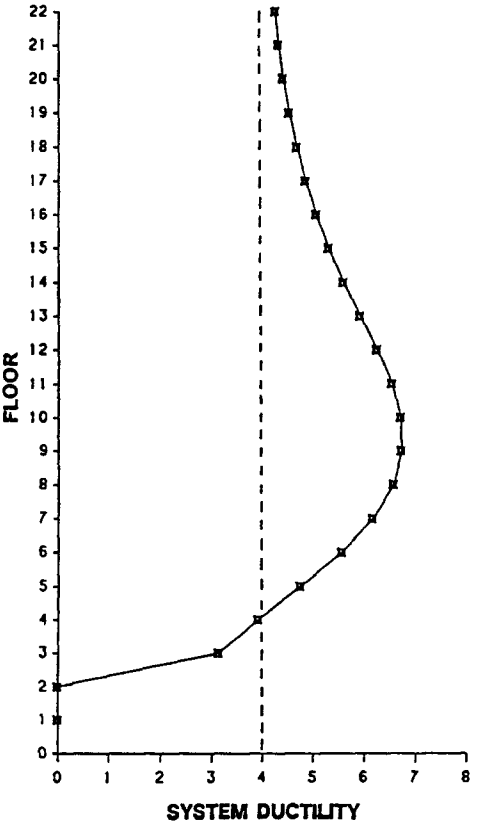

FIG. 11. System Ductility in GCS' X-Direction

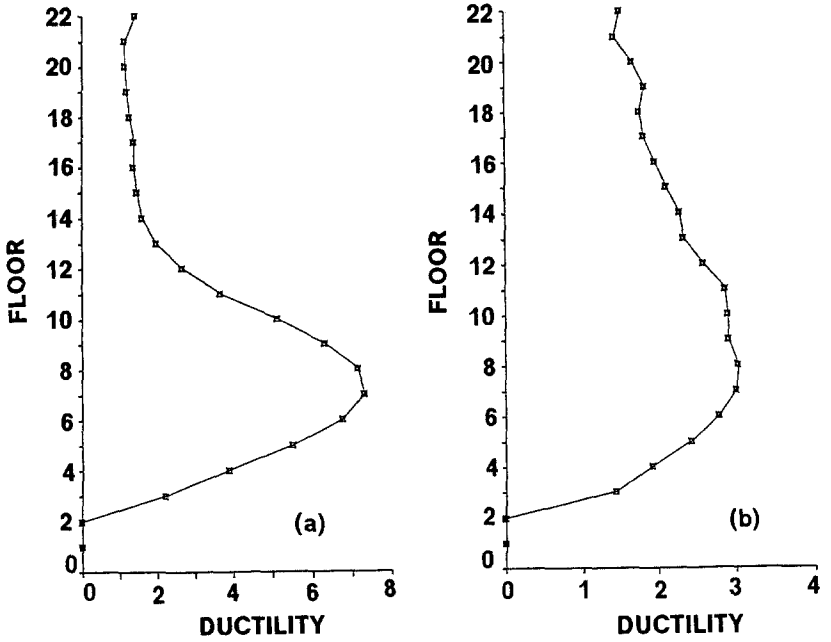

FIG. 12. Average Ductilities: (*a*) for Long-Direction Girders; and (*b*) for Short-Direction Girders

system ductility of a floor in the GCS' X-direction is defined as a ratio of maximum floor displacement in the X-direction at the mass center during 20 s of earthquake to that floor displacement when member 1413-1414 reaches its critical load.

System ductilities are shown in Fig. 11. Compared to design ductility 4 for this building, the ductilities based on present calculations are larger than 4. The average ductility of long-direction girders on each floor is plotted in Fig. 12(*a*). The average ductility of long-direction girders on a certain floor is obtained by averaging ductilities of all long-direction girders with ductilities greater than or equal to one on that floor. Figure 12(*a*) shows that long-direction girders with larger deformations are at the lower part of the building, and average ductilities on floors 4–10 are greater than 4. It implies that girders located in this weak zone, floors 4–10, may fail and lose their load-carrying capacities if they lack sufficient ductility. The average ductility of long-direction girders for each floor is greater than 1 except on floors 1 and 2. This means that most long-direction girders in the building have severe inelastic deformation. Similarly, the average ductility of short-direction girders for each floor is plotted in Fig. 12(*b*). Here the average ductility of short-direction girders for each floor is less than 4. Therefore, it is evident that the ductility requirement of long-direction girders in the lower part (Floors 4–10) of the building is greater than that of short-direction girders. Note that columns on floors 8–22 are not beyond the elastic limit for the present analysis.

With Girders' Failure Ductilities and Without Columns' Local Bucklings

Two cases are investigated: (1) Failure ductilities for long-direction girders and short-direction girders with a value of 4; and (2) failure ductilities for

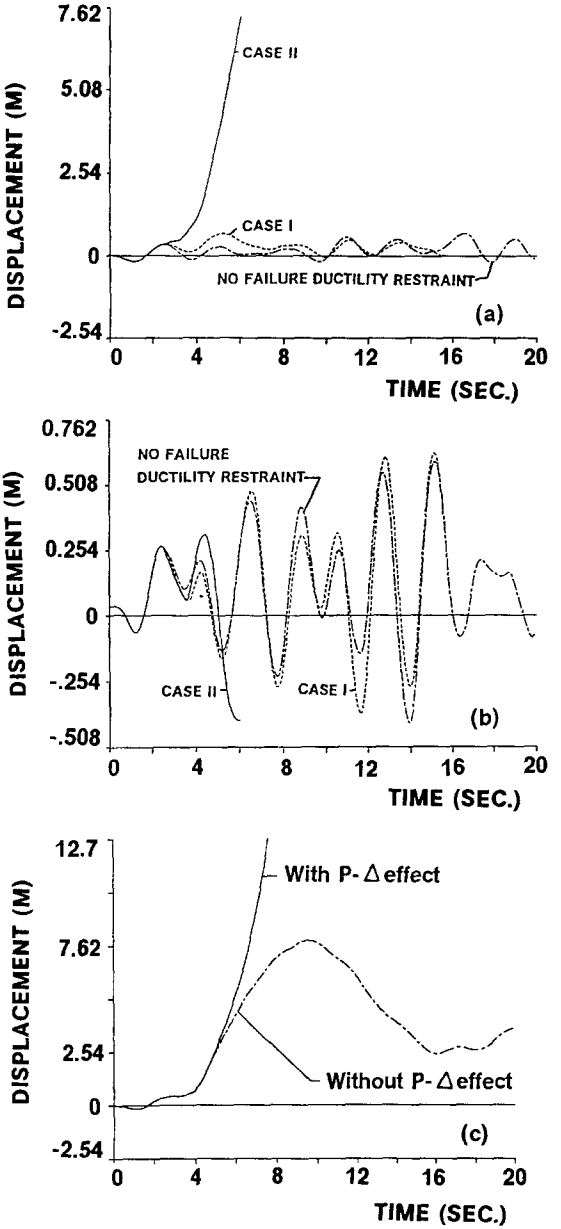

FIG. 13. Comparison of Translational Response at Top-Floor Mass Center: (*a*) in GCS′ *X*-Direction; (*b*) in GCS′ *Y*-Direction; and (c) With and Without *P*-Δ Effect

long-direction girders and short-direction girders with a value of 3. In both cases, the deformations of bracing members and columns are not restrained. The results of cases 1 and 2 are shown in Figs. 13(*a*) and 13(*b*), corresponding to the translational responses in the top floor mass center GCS′ *X*- and *Y*-

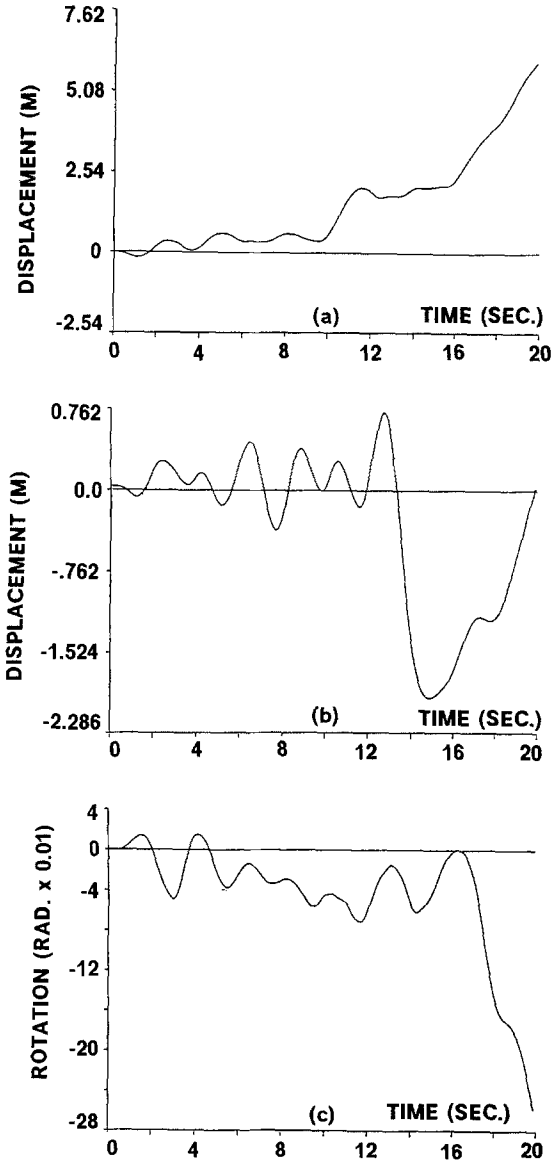

FIG. 14. Responses at Top-Floor Mass Center with Consideration of Failure Ductilities of Girders and Local Bucklings of Columns: (*a*) Translational Response in *X*-Direction; (*b*) Translational Response in *Y*-Direction; and (*c*) Torsional Response in *Z*-Direction

directions, respectively. Structural responses for case 2 increase significantly from the 4th s to the 6th s and are much larger than those for case 1. By implication, the smaller girders' failure ductilities underlie the larger structural responses. When the girders reach their failure ductilities, their internal force is released and redistributed to adjacent columns and bracings. Thus,

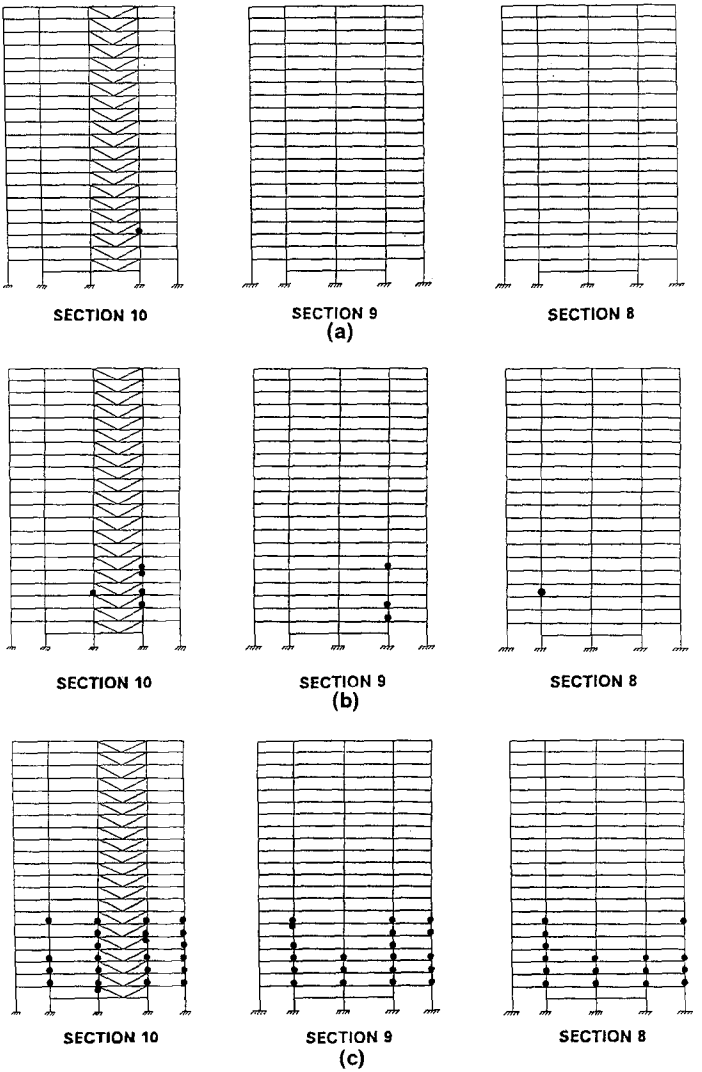

FIG. 15. Column Local Buckling Locations: (*a*) Time = 5 s; (*b*) Time = 10 s; and (c) Time = 15 s

the column ends may yield due to redistributed forces from ductile-failed girders as well as additional story shear from buckled bracing members. It is evident that a structure with girders of low failure ductility could easily collapse if its columns are not strong enough. Therefore, girder ductility and column strength are keys to the collapse behavior of a structure. Since several local buckled columns have been observed in the remaining building C, it is believed that structural collapse is attributed to not only ductile-failed girders but also local buckled columns. Therefore, structural responses for case 2 cannot conclude the actual collapse behavior of the building. Most of their yielding columns for case 2 are located on floors 4, 5, 6, and 7. This

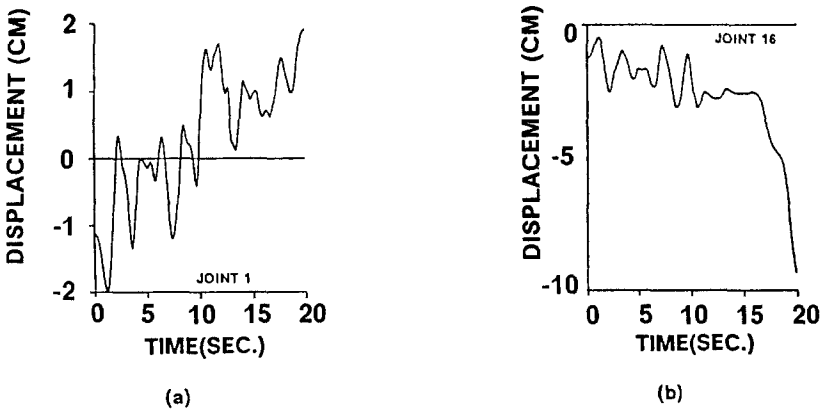

FIG. 16. Vertical Displacement on Top Floor: (*a*) at Column Line Number 1; and (*b*) at Column Line Number 16

is because the average ductility of long-direction girders [Fig. 12(*a*)] on floors 4–7 is greater than 3. Responses in the top-floor mass center GCS' X-direction for case 2 with and without consideration of structural geometric stiffness are compared in Fig. 13(*c*). This comparison shows that building collapse will not occur if structural geometric stiffness is not considered but will occur if structural geometric stiffness is considered. Therefore, P-Δ effect can help explain column yield in particular and collapse behavior in general.

With Girders' Failure Ductilities and Columns' Local Bucklings

Failure ductilities for long-direction girders and short-direction girders are assumed to be 4; 50% of residual axial strength and 50% of residual bending strengths are assigned to columns with consideration of local buckling. Results shown in Figs. 14(*a*), 14(*b*), and 14(*c*) correspond to translational responses in the top-floor mass center GCS' X- and Y-directions and torsional response in the GCS' Z-direction, respectively. Displacement in the positive X-direction increases dramatically from 10 s to 12 s, and in the negative Y-direction from 13 s to 15 s. Significant rotation develops in the negative Z-direction from 16 s to 20 s, with a maximum value of about 14.5°. Torsional effect emerges as a major factor in the collapse of this building. Displacement in the positive X-direction has a maximum value of about 5.969 m (235 in.). Local buckling of columns and weakening of girders result in significant story drift and increased P-Δ effects. A failure mechanism is in place that leads to collapse of the building. Local buckling columns projected at times equal to 5, 10, and 15 s are shown in Figs. 15(*a*), 15(*b*), and 15(*c*), respectively. The first column buckled locally is member 1805-1705 on floor 4 [Fig. 15(*a*)] at a time equal to 4.9 s, consistent with field observations at building C. Due to load redistribution effect, local bucklings occur at adjacent columns. At a time equal to 15 s, all columns except those in section *h* buckled locally on floors 2, 3, and 4. As columns lost their axial and bending rigidities, the building tilted in the positive X-direction and rotated in the negative Z-direction. Vertical displacements corresponding to floor 22 along column lines 1 and 16 are plotted in Fig. 16. Tilting effect is significant, especially after 15 s.

CONCLUSIONS

Hysteretic behavior was studied in order to assess inelastic capacity of structural components and to develop hysteresis rules. Rules have been established for bracing members and truss-type girders. An analytical model simulates the hysteretic behavior of local-buckled columns subjected to cyclic axial load and biaxial end moments.

Extensive inelastic analyses of the building were performed by three-dimensional seismic input, including vertical ground excitation with P-Δ effect, from actual Mexico City earthquake records. Most girders in the building exhibited severe inelastic behavior. System ductilities for floors 4–22 are greater than the building's design ductility of 4.

Weak zones in the structure are identified as follows: Average ductilities of long-direction girders for floors 4–10 are greater than 4; average ductility of short-direction girders on each floor is less than 4; most yielded columns are on floors 2–4. Earliest local-buckled columns are located on the 4th floor, which is consistent with field observations at one of the two remaining buildings.

Due to load redistribution effects from ductile-failed girders in weak zones, local bucklings occurred at adjacent columns on floors 2–4. Most columns on floors 2–4 then lost their load-carrying capacities and rigidity, causing the building to tilt and rotate. As a result, more columns on floors 5–7 developed local buckling and more bracing members buckled. Ductile breakdown of girders combined with local buckling of columns in the lower part of the building to create a failure mechanism that caused significant story drift, building tilt, increased P-Δ effect, and structural collapse.

From experimental and analytical studies of the Pino Suarez building, one could improve the structure's performance by: (1) Using a symmetric structural plan in order to avoid torsional motions; (2) using solid welds, instead of stitch welds, for the boxed angle web members to enhance the ductility of open-web girders; and (3) using strong columns for not having plastic hinges and local buckling developed in the columns.

ACKNOWLEDGMENTS

This research work is supported by the National Science Foundation under grant CES 8706531. The project was conducted through collaborative efforts between the University of Missouri-Rolla and Lehigh University. Significant assistance was received from Oscar DuBuen for field observation and engineering design data. Computing time was granted by the Cornell National Supercomputer Facility (CNSF). All support for the research is gratefully acknowledged. The findings and conclusions are the opinions of the writers.

APPENDIX I. REFERENCES

Allowable stress design manual of steel construction. (1989). Ninth Ed., American Inst. of Steel Constr., Chicago, Ill.

Black, R. G., Wenger, W. A. B., and Popov, E. P. (1980). "Inelastic buckling of steel struts under cyclic load reversals." *Report No. UCB/EERC-80140*, Earthquake Engrg. Res. Ctr., Univ. of California, Berkeley, Calif.

Chen, C. C. (1991). "Approaches to improve seismic resistance of steel building frames," PhD dissertation, Lehigh Univ., Bethlehem, Pa.

Chen, W. F., and Sugimoto, H. (1987). "Cyclic analysis of tubular beam-columns and frames." *Report No. CE-STR-87-11*, Purdue Univ., West Lafayette, Ind.

Cheng, F. Y. (1980). "Inelastic analysis of 3-D mixed steel and reinforced concrete

seismic building systems." *Computational methods in nonlinear structural and solid mechanics*, Pergamon Press, Elmsford, N.Y., 189–196.
Cheng, F. Y. (1985). "Matrix methods of structural analysis II." *Class Notes, CE 428*, Univ. of Missouri-Rolla, Rolla, Mo.
Cheng, F. Y., and Kitipitayangkul, P. (1979). "Investigation of the effect of 3-D parametric earthquake motions on stability and elastic and inelastic building systems." *NTIS No. PB80-176936*.
Cheng, F. Y., and Ger, J. F. (1992). "Inelastic response and collapse behavior of steel building structures subjected to multicomponent earthquake excitations." Civil Engineering Studies, Structural Series 92-30, Univ. of Missouri-Rolla, Rolla, Mo.
Ger, J. F. (1990). "Inelastic response and collapse behavior of steel tall buildings subjected to 3D earthquake excitations," PhD dissertation, Univ. of Missouri-Rolla, Rolla, Mo.
Ger, J. F., and Cheng, F. Y. (1992). "Collapse assessment of a tall steel building damaged by 1985 Mexico earthquake." *Proc. of the Tenth World Conference on Earthquake Engineering*, Madrid, Spain, 51–56.
Ger, J. F., and Cheng, F. Y. (1993). "Postbuckling and hysteresis models of open-web girders." *J. Struct. Engrg.*, ASCE, 119(3), 831–851.
Jain, A. K., Goel, S. C., and Hanson, R. D. (1980). "Hysteretic cycles of axially loaded steel members." *J. Struct. Div.*, ASCE, 106(8), 1777–1795.
Kannan, A. E., and Powell, G. H. (1973). "DRAIN-2D, A general purpose computer program for dynamic analysis of inelastic plan structures." *Report No. EERC 73-6 EERC 73-22*, Univ. of California, Berkeley, Calif.
Liew, J. Y. R., Shanmugam, N. E., and Lee, S. L. (1989). "Behavior of thin-walled steel box columns under biaxial loading." *J. Struct. Div.*, ASCE, 115(12), 3076–3094.
Osteraas, J., and Krawinkler, H. (1989). "The Mexico earthquake of September 19, 1985—Behavior of steel buildings." *Earthquake Spectra*, 5(1), 51–88.
Saiidi, M., and Sozen, M. A. (1979). "Simple and complex models for nonlinear seismic response of reinforced concrete structures." *Report No. 465*, Civ. Engrg. Studies, Univ. of Illinois at Urbana-Champaign, Urbana, Ill.
Zhou, S. P., and Chen, W. F. (1985). "Design criteria for box columns under biaxial loading." *J. Struct. Div.*, ASCE, 111(12), 2643–2658.

APPENDIX II. NOTATION

The following symbols are used in this paper:

$E1$ = elastic stiffness of short-direction girder;
$E2$ = inelastic stiffness of short-direction girder;
F_y = yielding stress;
M_{cr} = critical moment;
M_p = plastic moment;
M'_p = reduced plastic moment;
M_x = moment in x-direction;
M_y = moment in y-direction;
P_y = yielding load;
P_{cr} = critical axial load;
θ_{cr} = critical rotation;
β = residual bending strength factor;
β' = residual axial strength factor;
δ_{max} = maximum deformation;
δ_y = critical deformation; and
μ_d = failure ductility.